Characterization of a Thg1-Like Protein in *Dictyostelium discoideum*

A Senior Honors Thesis

Presented in partial fulfillment of the requirements for graduation with research distinction in the undergraduate colleges of The Ohio State University

By

Andrew Nguyen

The Ohio State University
April 2021

Project Advisor: Dr. Jane E. Jackman, Department of Chemistry and Biochemistry

Abstract

The $tRNA^{His}$ guanylyltransferase (Thg1) is an essential, highly conserved enzyme in many eukaryotes, and the cytoplasmic role for members of this enzyme family has been well established and extensively studied; the Thg1 enzyme is well known to use an unusual 3'-5' polymerase activity to play an essential role in maturation of nucleus-encoded $tRNA^{His}$. However, recent studies in the slime mold *Dictyostelium discoideum* (Ddi-) have revealed new functions for Thg1 family members in mitochondrial metabolism that are not completely understood. This mold encodes two mitochondrial Thg1-Like Proteins (TLPs) that catalyze RNA modification by incorporating nucleotides in the same 3'-5' direction to distinct tRNA substrates, yet it does not encode the highly conserved RNase P in its mitochondria. I hypothesize that mitochondrial Thg1 homologs interact with other mitochondrial tRNA processing enzymes to catalyze their important functions, and possibly other functions that are distinct from the other more well-studied cytosolic functions of these enzymes. To test this hypothesis, I investigated the proteins that one of these homologs, DdiTLP2, interacts with during its catalysis of mitochondrial $tRNA^{His}$ (mt-$tRNA^{His}$) maturation by using an epitope tag and immunoprecipitation. The epitope tagged protein was analyzed *in vitro* and *in vivo*, where an efficiency defect was discovered in both cases. Additionally, we have optimized a development assay for a deletion strain of DdiTLP2, discovering that it demonstrates a developmental defect.

Introduction

Throughout biology, we have discovered common themes that exist across all domains of life. One such theme is the transfer of genetic information in cells, which is often known as the central dogma of molecular biology. In every cell, enzymes work to transcribe DNA to mRNA and translate mRNA into proteins. This universal process enables life, as it efficiently and precisely synthesizes many proteins that make life possible. At the center of this process lies tRNA, the nucleic acid responsible for bringing amino acids to the growing peptide chain. This specific step in the central dogma, translation, is unique due to the participation of a separate and distinct nucleic acid to bridge RNA and protein sequences. tRNA is often overlooked due to its exclusion from the generic explanation of the central dogma (DNA to mRNA to protein), yet its role in the cell is extremely nuanced and essential. There are numerous interactions and enzymes involved in translation, and incredible specificity is required between all these macromolecules for them to work correctly. This specificity can be rooted in a multitude of areas, including genetic differences in the nucleic acid sequences that allow them to be distinguished properly and post-transcriptional modifications on the nucleic acids. Such specificity allows for tRNA recognition by the correct synthetase and subsequent aminoacylation, resulting in the addition of amino acids to the growing peptide chain and proteins synthesis[1–6].

This work will focus on tRNA, a molecule that is subject to significant processing prior to its use in translation, including being heavily decorated with post-transcriptional modifications[7,8]. These processing events occur all throughout the cloverleaf structure of tRNA, from the 5' end to the 3' end, producing a mature tRNA[7,8]. During tRNA maturation, there are a multitude of processing reactions that must occur correctly, including but not limited to: removal of 5' or 3' leaders by exo/endonucleases, intron splicing, addition of the 3’ CCA sequence, and tRNA modifications to

pseudouridine[7–9]. Interestingly, one of the RNA processing reactions that has been recently described involves an unusual chemistry for nucleotide addition. Even though canonical synthesis of all RNAs by transcription occurs in the 5'-3' direction, the discovery that a G_{-1} nucleotide can be added to the 5'-end of $tRNA^{His}$ by the enzyme $tRNA^{His}$ guanylyltransferase (Thg1) revealed that nucleotide addition in the non-canonical (3'-5') direction is also possible[1,10,11].

Thg1 was first discovered in the yeast *Saccharomyces cerevisiae* (yThg1), where it catalyzes the addition of a G_{-1} nucleotide to the 5' end of cytoplasmic $tRNA^{His}$ (Figure 1B)[1,10,11]. This non-templated addition does not follow Watson-Crick base-pairing rules, as the G nucleotide is added across from the A_{73} residue[10,11]. The discovery of yThg1 led to further research into this non-canonical nucleotide addition, revealing the near universally conserved nature of Thg1 in eukaryotes[12–14]. Thg1 has also been discovered in bacteria and archaea, although the enzyme is not conserved in these domains[12–14]. Still, bacteria and archaea encode the G_{-1} nucleotide in their gene for $tRNA^{His}$ and retain this nucleotide after 5' end processing[15,16]. In fact, the inclusion of the G_{-1} nucleotide is a universally conserved hallmark of mature $tRNA^{His}$ across all domains of life[12]. It is required for proper recognition by the cognate histidyl-tRNA synthetase (HisRS) and subsequent aminoacylation[1–6]. Once the yeast gene was identified, searches for homologs in other organisms led to the discovery of the Thg1 superfamily of enzymes. This superfamily consists of both Thg1 and Thg1-Like Proteins (TLPs), enzymes that are distinct from Thg1 in terms of sequence but catalyze a similar 3'-5' nucleotide addition reaction[11,17–21]. TLPs are also different from Thg1 in that they do not have the ability to catalyze non-Watson-Crick addition; instead, they prefer to synthesize Watson-Crick base-paired nucleotides with RNA substrates[14,17,18]. These TLPs have been discovered across all domains of life, such as the

archaeal species *Methanosarcina barkeri*, the bacterial species *Myxococcus xanthus*, and the eukaryotic species *Dictyostelium discoideum*[12]. TLPs are generally conserved in bacteria and archaea, as all bacteria and archaea that have been researched contain one TLP and no Thg1[10,12–14]. Eukaryotes can contain both a Thg1 and a TLP[10,12–14].

This work will focus on *Dictyostelium discoideum* (Ddi-) as a model system to investigate the functions of its four Thg1 family enzymes, especially the two that are localized to the mitochondria. This organism encodes one Thg1 enzyme, DdiThg1, and three Thg1-Like Proteins (TLPs), DdiTLP2-4[13,22]. Of the four Thg1 family enzymes, only one has an unknown function[22]. The function of DdiThg1 was readily predicted based on its homology to *S. cerevisiae* Thg1, and its role in the addition of a G_{-1} nucleotide to cytosolic $tRNA^{His}$ was previously confirmed[13]. DdiTLP2 was discovered to have a similar role to DdiThg1, but occurring in the mitochondria, where it adds a G_{-1} nucleotide to mitochondrial $tRNA^{His}$ (mt-$tRNA^{His}$)[22]. DdiTLP3 was found to catalyze mitochondrial tRNA editing on the 5' end, acting on many different mt-tRNAs while DdiThg1 and DdiTLP2 only act on one specific tRNA[13,14,22,23]. The function of DdiTLP4 remains unknown, although its activity has been demonstrated with multiple tRNAs and non-tRNAs *in vitro*[12,22,24–26]. Of these four enzymes, three fourths of them have been found to be essential to the survival of the cell, where DdiTLP2 is not essential[2,22,27–29]. Interestingly, DdiTLP2 naturally exhibits an incomplete addition of G_{-1} to mt-$tRNA^{His}$, as its innate efficiency only allows for addition of the G_{-1} nucleotide to 69% of mt-$tRNA^{His}$ [22]. This is distinct from DdiThg1, which adds the G_{-1} nucleotide to all $tRNA^{His}$ in a cell[10,13]. In addition, DdiTLP2 has been found to be non-essential to the survival as the cell even if it supplements the growth of the mold, as a deletion strain of DdiTLP2 has been previously found to only demonstrate a

vegetative growth defect with no other phenotypic changes between the DdiTLP2Δ strain and the wild type strain[22].

Still, the basic functions of the two *D. discoideum* mitochondrial TLPs may not be their only role within the cell. Mitochondrial TLPs are involved in broader tRNA maturation pathways whose players, including the full complex of enzymes that catalyze mitochondrial tRNA 5'-end processing, have not yet been fully identified. The complexity of tRNA editing and the many intertwined processes suggest that TLPs may interact with other tRNA modification enzymes or tRNAs during its catalysis of the G_{-1} nucleotide addition to $tRNA^{His}$ (Figure 1B) [7,8]. Moreover, the mitochondrial phenotypes and consequences of inactivation of mitochondrial Thg1/TLP family enzymes have not been completely assessed, despite the fact that vertebrate Thg1 enzymes are dual-targeted to both cytosol and mitochondria, as verified in humans[30–34]. Therefore, how these enzymes contribute to mitochondrial health and human disease, including the possibility of alternative RNA-processing or repair activities catalyzed by these enzymes, is not known.

In this project, we aim to identify candidate proteins for additional mt-tRNA processing activities by identifying the proteins that wild-type DdiTLP2 associates with, using an engineered epitope tagged DdiTLP2 enzyme that will be expressed in *D. discoideum* and used to co-immunoprecipitate interacting proteins. This will be accomplished by cloning, expressing, and purifying an epitope tagged DdiTLP2, then analyzing the activity of the tagged enzyme with a phosphatase protection assay. If the tag is shown to have no effect on the activity of the enzyme, the epitope tagged DdiTLP2 can be expressed into *D. discoideum* cells, where the proteins associated to DdiTLP2 can be identified using the immunoprecipitation approach targeting the engineered epitope tag.

Chapter 1: Determination of the efficiency of epitope tagged DdiTLP2 in catalysis of G_{-1} nucleotide addition to the 5' end of mitochondrial $tRNA^{His}$.

In all organisms, tRNA undergoes extensive maturation processes prior to the addition of an amino acid to the growing peptide chain. These processes vary from 5' processing by RNase P, 3' processing by endo/exonucleases, splicing of introns, or addition of the conserved 3' CCA sequence[7–9]. Due to the interconnected nature of these processes, it is reasonable to believe that the enzymes that catalyze each of these reactions may interact with each other in the cell, such as through physical clustering in the nucleolus as observed in eukaryotic cells. Here, we will focus on the possible interactions between other tRNA processing enzymes and DdiTLP2. This TLP was chosen due to its non-essential role in the cell. Of the three TLPs present in *D. discoideum*, this enzyme is the only one that is not essential to the cell's survival, as previously confirmed by sequencing of the mt-$tRNA^{His}$ from a deletion strain of DdiTLP2[22]. This deletion strain was produced using a blasticidin S-resistance cassette, where a reproducible and statistically significant vegetative growth defect was observed[22]. Total RNA was extracted from these DdiTLP2Δ cells, and following circularization of the tRNA, RT-PCR was used to determine that there all the mt-$tRNA^{His}$ were missing the signature G_{-1} nucleotide that is normally added by DdiTLP2[22]. This contrasts with the G_{-1} observed on 69% of mt-$tRNA^{His}$ seen in wild type *D. discoideum*[22]. These two unique features of DdiTLP2, being non-essential to the survival of the cell and incomplete addition to the substrate tRNA, has not yet been observed in any other enzyme within the Thg1 superfamily[14,22]. As such, we believe that characterization of DdiTLP2 is essential to understanding the Thg1 superfamily. In addition, the incomplete addition of G_{-1} to mt-$tRNA^{His}$ leads us to believe that DdiTLP2 may serve additional purposes in tRNA maturation processes.

To test this hypothesis, we chose to add an epitope tag to DdiTLP2 for immunoprecipitation. A FLAG tag was chosen for this purpose, given its small size (24 nucleotides) and ready availability of high quality anti-FLAG antibodies for use in immunoprecipitation procedures[35]. The long-term goal of this work is to isolate the DdiTLP2 from the cell, add a crosslinking reagent to covalently link proteins that interact with DdiTLP2, immunoprecipitate the resulting conglomeration, and identify any co-purifying proteins using mass spectrometry. I expect that this procedure would allow us to identify RNA processing proteins that interact with DdiTLP2, as well as possibly to identify other proteins that have not previously been associated with tRNA, thus providing insight into other purposes of DdiTLP2 in the cell. Due to the plethora of tRNA maturation processes and post-translational modifications in the cell, such an immunoprecipitation would provide a framework for us to research these interactions more stringently. As the first step toward carrying out this approach, I sought to evaluate the effect of the epitope tag on the catalytic efficiency of DdiTLP2, which could adversely affect protein folding or post-translational modifications, despite the relatively small size of the FLAG epitope sequence.

Results

Cloning, expression and purification of C-terminal epitope tagged DdiTLP2

To test how the presence of an epitope tag affects the activity of DdiTLP2 enzyme, I aimed to create DNA constructs that would incorporate a Flag-tag on either N or C termini of the DdiTLP2 gene when expressed and purified as a recombinant protein. We were unsure which terminal addition would significantly impact enzyme efficiency, so both constructs were independently synthesized (Figure 2A). I designed primers for Phusion PCR, which amplifies the

wild type DdiTLP2 gene with primers that introduce an additional Flag tag sequence. This gene is in the AVA421 plasmid which contains an N terminal His_6 tag, ampicillin resistance, and an IPTG inducible promoter. The resulting sequence was circularized by ligation for subsequent transformation into XL1-Blue cells to recover clones. After restriction screening by EcoRI and PstI to identify positive candidates, the addition of a Flag tag onto the DdiTLP2 gene could be confirmed by sequencing. After these procedures, addition of the C-term tag was successful, while the correct N-term tag was not obtained (Figure 2A). The C-terminal Flag plasmid was then transformed into Rosetta pLysS cells which was grown over two days, producing a 1L culture. Once the cells in the 1 L culture have reached exponential growth, the tagged protein was produced with IPTG overexpression of the *lac* operon. Following overexpression, the cells were lysed using a French Press, the Flag-tagged DdiTLP2 was purified using immobilized metal ion chromatography targeting the His_6 tag and quantified using a Bradford assay (Figure 2B). The final concentration of the protein was 8.44 mg/mL and approximately 900 μL of protein are obtained.

Immunoblotting of the Flag-tagged DdiTLP2

The resulting protein from purification was then analyzed to confirm the presence and activity of a Flag tag. A Western blot was performed for the detection of the epitope tag. We used an anti-Flag antibody, where the primary and secondary antibodies were conjugated to each other. This antibody was generated from a mouse. Through this immunoblotting process, the presence and strong activity of the C terminal Flag tag were confirmed (Figure 3 A-C).

Determination of the catalytic efficiency of the Flag tagged DdiTLP2

The activity of the Flag tagged DdiTLP2 was analyzed using an *in vitro* phosphatase protection assay, where the activity of tagged and non-tagged DdiTLP2 enzymes were compared[11]. In this assay, 5'-P^{32} mt-$tRNA^{His}$ is reacted with the tagged and non-tagged DdiTLP2 (Figure 4A). The reaction is then quenched with RNase A and subsequently treated with a phosphatase, specifically CIP. These steps separate 5' phosphates from the mt-$tRNA^{His}$, resulting in separation of the 5' radiolabeled phosphate or a seven-nucleotide fragment containing the radiolabeled phosphate. This fragment can only be generated by G_{-1} addition onto the 5' end of the mt-$tRNA^{His}$. This assay was run both as an endpoint and as a time course assay. The endpoint assays revealed that the wild type DdiTLP2 produced approximately twice the amount of mature mt-$tRNA^{His}$ as the Flag tagged DdiTLP2 (Figure 4B). The time course assays revealed an approximately 22-fold difference in G_{-1} addition between tagged and non-tagged DdiTLP2, where tagged DdiTLP2 was less active (Figure 4C-E). This was determined using a different kinetic method for each enzyme. The wild type DdiTLP2 product formation data was fit well by a single exponential rate equation to determine the k_{obs}, so the rate constant for wild type DdiTLP2 was determined directly from the equation. The Flag tagged DdiTLP2 could not be fitted in this manner, as the observed data points did not follow the single exponential rate equation. As a result, the method of linear initial rates was used to calculate the k_{obs} for the tagged DdiTLP2. This method uses the linear initial rate and the maximum percentage of product formation to calculate the k_{obs}.

N-terminal Flag tagged DdiTLP2 does not recover the vegetative growth defect of DdiTLP2Δ

Using Phusion PCR, we were able to obtain a DNA construct with an N-terminal Flag tag on DdiTLP2 in a *D. discoideum* shuttle vector under control of the *ACT15* constitutive promoter for expression in *D. discoideum*. This construct was electroporated into the DdiTLP2Δ strain, and subsequent cell growth was observed (Figure 5A). A growth curve of the wild type *D. discoideum*, DdiTLP2Δ strain, and of the N-terminal Flag tagged DdiTLP2 strains was obtained, and an obvious initial growth defect was observed that is consistent with previous results. However, the vegetative growth defect of the DdiTLP2Δ strain was not observed for any of these strains; further experiments are required to understand why this growth defect was not recapitulated, whether it be changes in the strain after long term storage or slightly different growth conditions than those described previously. One possible reason for the inability of the epitope tagged DdiTLP2 to completely complement the growth defect could be because of low expression of this protein, possibly caused by the presence of the FLAG epitope. Thus, we also wanted to measure the expression of this Flag tagged DdiTLP2. This was done with a Western blot, where expression of the enzyme was confirmed (Figure 5B-D).

Discussion

In this chapter, I described how I was able to construct and test one of the two DdiTLP2 epitope tagged proteins that is needed to carry out the immunoprecipitation experiment to identify interacting proteins. Construction of the epitope tagged DdiTLP2 began with slight difficulties in the mutagenic PCR protocol. Phusion PCR was chosen due to its ability to add short fragments into an existing DNA plasmid. This is ideal for the addition of a Flag tag, as its

sequence is only 24 nucleotides long and could be designed to contain enough G and C residues to ensure optimal primer design[35]. This cloning strategy was successful for the addition of the Flag tag onto the C terminus of the DdiTLP2. Still, we were unable to generate a DdiTLP2 with the Flag tag on the N terminus. As can be seen from the agarose gel following PCR (Figure 2A), a DNA fragment with the expected size was generated from both PCR reactions. Since the expected band did appear on the gel, the ligation reactions were carried out, and the resulting DNA was transformed into competent cells and growth was observed on ampicillin plates. However, the resulting DNA from these cells never contained the desired N terminal epitope tagged DdiTLP2, as confirmed by sequencing. Subsequent gel extractions and altered primer annealing temperatures were also unsuccessful, as any strain that produced viable bacteria following ligation and transformation did not contain the correct sequence, again confirmed by sequencing results. Future studies involving *in vivo* assays will further analyze N terminal Flag tagged DdiTLP2, since these *in vitro* methods were ultimately unsuccessful. Future studies will also require an alternative method for generating this DNA construct, leading to a more complete picture of DdiTLP2.

Following these cloning procedures, the C-terminal Flag tagged DdiTLP2 was purified. The C terminal Flag tagged DdiTLP2 gene was transformed into Rosetta pLysS cells, where the T7 promoter controlling expression of DdiTLP2 was induced using IPTG. The resulting protein was purified using an immobilized metal ion affinity chromatography (Figure 2B). To confirm that the purified protein contained the FLAG epitope that was introduced by mutagenesis, a Western blot was performed. Even as we intentionally placed the tag on the terminus of the peptide sequence, there was a chance that the folded conformation adopted by the protein could result in degradation of the protein, which could lead to loss of the epitope tag. However, the western blot

confirms that the tag is present in very high amounts (Figure 3C). This will be helpful for future immunoprecipitations, as the presence of the Flag tag allows for immunoprecipitation of DdiTLP2.

The purification of the epitope-tagged protein allowed us to continue and test the activity of the DdiTLP2 enzyme that contains this additional sequence. It was important to confirm that the tag did not significantly interfere with the activity of the enzyme, as a significant reduction in activity would mean that the possible interactions of the enzyme and other proteins would also be affected, resulting in an inaccurate immunoprecipitation. The activity decrease could have induced an increase or decrease in protein-protein interactions, so we would want to see the same activity in our Flag tagged DdiTLP2 as in wild type DdiTLP2. This led us to the phosphatase protection assay, a common method used in our laboratory to assess the activity of Thg1 and TLPs[11]. The resulting efficiency difference between the Flag tagged DdiTLP2 and wild type DdiTLP2 led us to a difficult decision. While a 22-fold decrease in rate associated with presence of the epitope tag could not be ignored, it was small enough for us to consider moving forward with the project. Although this is not known for TLP2, it is possible that even a sub-optimally active protein could still fulfill the biological function of the wild-type protein. This is due to the safeguards that are present in a typical cell that can sometimes buffer the cell from detrimental changes in protein expression. In a cell, some proteins are produced in excess, as the production of exact stoichiometric quantities would harm the cell should the production of that protein be affected. In addition, there are many post-translational modifications *in vivo* that cannot be replicated *in vitro*. It is possible that the presence of native modifications on the FLAG-tagged DdiTLP2 could help to compensate for the decreased activity of the enzyme, again leading to sufficient levels of activity *in vivo*.

To assess whether either of these mechanisms might be possible for DdiTLP2, we reasoned that if the growth defect of DdiTLP2 can be recovered by transforming Flag tagged DdiTLP2 into the DdiTLP2Δ strain, then the epitope-tagged protein could be used for IP experiments. To fully assess whether the tagged TLP2 recovers wild-type function, we would need to perform analysis of total RNA in cells expressing this protein and determine how much G_{-1} has been added to the mt-$tRNA^{His}$. If this number is not different statistically compared to the 69% previously observed in wild type *D. discoideum,* we would confirm that the C-terminal epitope tagged DdiTLP2 can be used in place of the wild-type protein to identify functional protein interactions[22]. Unfortunately, although the recombinant data were obtained for the C-terminally tagged protein, we were not able to obtain an equivalent C-terminal FLAG-tagged construct for expression in *D. discoideum*, due to similar cloning issues encountered earlier. However, we were able to obtain an N-terminal Flag tagged DdiTLP2 in the vector for expression in *D. discoideum* and decided to move forward with the growth complementation experiments, despite the mismatch in proteins being studied with each approach. As described before, if either of the tagged enzymes was able to revert the vegetative growth defect of the deletion strain, we would consider this evidence of the protein's function and appropriateness for use in the immunoprecipitation approach.

Unfortunately, this was not the case for N-terminal Flag tagged DdiTLP2. While we were never able to analyze the efficiency of this enzyme *in vitro*, the initial growth defect observed for the DdiTLP2Δ strain and the N-terminal Flag tagged DdiTLP2 indicate that there may also be problems with introducing a Flag epitope at this location of the protein. The western blot confirmed that the enzyme was expressed, so this could not have been the issue that led to an inability to complement the growth defect (Figure 5C). Still, of the two tested positions, we

consider it more likely that the N-terminal of the DdiTLP2 peptide sequence is not an optimal location to place the tag on. This tag sits inside of a mitochondrial targeting sequence on the N terminus, which is used to target this protein to the mitochondria and then is cleaved after protein import. The presence of this additional sequence at this location may interfere with protein folding or import and therefore be more likely to create a non-functional protein. This possible interference would be avoided on the C terminus. We hope that this bodes well for the recovery of the vegetative growth defect once we are able to obtain the necessary construct for C-terminal epitope tagged protein expression, but it will need to be assessed in future studies.

Chapter 2: Characterization of the development of *D. discoideum* using a development assay

As our knowledge about stem cells has increased, *D. discoideum* has been coined as "nature's stem cell." This status stems from the mold's ability to change form and aggregate as it is deprived of nutrients[36,37]. This aggregation and subsequent development cycle have been well established (Figure 6A)[36,37]. This mold begins as a single, vegetative amoebae that matures into a multicellular fruiting body[36,37]. Aggregation is induced by depriving the cells of nutrients, such as plating the cells onto plates composed of agar and a salt. The aggregation is mediated by a chemotaxis of cells towards a secreted cAMP signal, forming mounds[36]. These mounds will continue to aggregate and grow higher, such that eventually the mounds will fall over. The cells now form a slug structure, the next point in development. Aggregation will then continue in a similar fashion, where the cells will aggregate at one end point of the slug. Such an aggregation describes a culminant or Mexican hat, where there is a complete accumulation of cells at one end of the slug but a lack of verticality. If the cells do achieve verticality, where the cells have differentiated into stalk cells that support a spore head, the cells are in the fruiting body phase. For this work, the fruiting body will be considered the end of development. In the life cycle of *D. discoideum*, fruiting bodies will sporulate and produce more spores to restart the development cycle[36]. However, these spores are not observable at the same zoom as the aggregated structures, so they will not be considered here.

Interestingly, the development of the DdiTLP2Δ strain has not been described in any of our lab's previous work. Instead, the growth of the DdiTLP2Δ has been described, where the vegetative growth defect was observed. There was no morphological difference observed in the single cells when observed under a microscope, where the wild type AX2 cells and the DdiTLP2Δ both had

a circular shape and translucent appearance. The use of a development assay would provide a more complete picture of the growth of the DdiTLP2Δ strain. Here, I report on my comparison of the development of wild type *D. discoideum* and DdiTLP2Δ cells using a development assay.

Results

Optimization of the *D. discoideum* development assay

The development of *D. discoideum* has been well described and photographed using higher concentrations of cells grown over a short period of time[36]. However, due to the vegetative growth defect of the DdiTLP2Δ strain, we aimed to develop a new protocol where cells could be more readily compared, despite the slower growth phenotype associated with the TLP2Δ strain. We used the same buffers and plates as previously described, where the cells are washed in buffer to remove nutrients and plated on nutrient poor KK2 plates which are composed of agar and a salt. Still, the concentrations and growth times for these concentrations needed to be optimized. Concentrations ranging from 1 million to 5 million cells per 10 cm petri dish grown over one week provided the most useful data after development was complete. All four of the previously described structures in development – slugs, mounds, culminants, and fruiting bodies – were counted at various time points throughout the development assay. At each point, the plates were photographed under a microscope and a representative counting area was chosen for each image. This was done to reduce the counting burden for the assay and to ensure that we could see if any fruiting sprouted from outside the counting area but had a spore head inside the counting area. A 3 mm by 3 mm square was used as this counting area. Structures in each counting area were categorized into one of these four groups, and the percentage of structures in each stage was calculated. After one week of growth, there were no more significant changes to

these percentages. Any spores that were produced by either the wild type or DdiTLP2Δ strains following fruiting body formation were either unable to form mounds or formed mounds that were too small to be observed at the chosen magnification.

DdiTLP2Δ exhibits a developmental growth defect

In previous work, the DdiTLP2Δ strain was only found to have a vegetative growth defect that results in a slightly slower doubling time when grown in liquid media[22]. To test the same DdiTLP2Δ cells for their ability to undergo development, cultures were grown first in liquid media to obtain a sufficient cell count, and then on plates for development (Figure 6B, C). At the optimized concentrations of cells described above, the DdiTLP2Δ strain demonstrated a statistically significant developmental growth defect (Figure 6D). A significantly higher percentage of wild type cells reached the fruiting body stage, the largest structure that can be seen and the designated end point for the development assay. The DdiTLP2Δ strain had a significantly higher percentage of cells at each of the earlier development stages, except for mounds. At higher concentrations, the DdiTLP2Δ did demonstrate a small developmental defect, although it was not statistically significant. This defect may prove statistically significant over a larger sample size, but at the size seen in this experiment it was not significant.

Discussion

The development assay for *D. discoideum* has been well described in the past but has not been used to study the DdiTLP2Δ strain that was the focus of this work. These previous assays have utilized approximately 10 million cells per 10 cm Petri dish, where the cells will undergo rapid development, completing the entire process in 24-48 hours[36]. This did not allow for a sufficiently sensitive development assay to detect smaller differences between wild type vs. mutant cells that

might only be visible at certain times during the process, as access to a microscope was limited at odd hours of the day. Furthermore, the vegetative growth defect of the DdiTLP2Δ strain did not allow for this large number of cells to be easily grown. As a result, we chose to decrease the number of plated cells used to start the assays. We believed that this modification would allow us to photograph the cells throughout their development, ensuring that we would capture the cells at the moment development was complete, and at multiple stages in between.

The decreased initial cell counts also affected the aggregation of the cells. As there were less cells on the plate, we reasoned that the cells would develop slower than in the previously described development assays. We believed that with fewer cells on the plate, the time required for chemotaxis would increase and slow the development cycle. This suspicion was confirmed, as plates with 1-5 million cells finished development over 7 days. The lower cell counts described here would be useful in future development assays, as the longer development time and decreased aggregation allowed us to obtain a more rigorous development assay. We would also be able to document the growth of *D. discoideum* throughout the development cycle, although these data may not be as important as the endpoint data. This is because we were most interested in the percentage of cells that reached each developmental stage.

The other main difference between plates with higher cell counts and those with lower counts was the size of the structures that were observed. On plates with higher counts, the structures observed were much bigger in size, resulting in more subjective counting. In many cases, the structures on these plates extended past the edge of the chosen counting area, regardless of the specific part of the image. It was difficult to discern which structures to count and which to ignore, as we only wanted to count those which were in a set area for standardization. This was especially difficult for fruiting bodies, as the stalk would often extend through half of the

designated counting area. It was also difficult to ensure that all structures in each area were counted, as fruiting body stalks would overlap inside the counting area. It was then hard to discern slugs from fruiting bodies, and if a fruiting body sprouted from inside the counting area or not. Interesting, a similar number of structures were observed on plates with lower cell counts, yet the structures were much smaller. We had expected to observe a smaller number of structures due to the lower cell count, but it seems that the greater distance between cells only affected the size of the structures. This difference greatly aided the standardization of the counting protocol. It was easier to maintain accuracy and precision when counting these structures, as very few of them extended far into or out of the counting area. The structures also were separated in the counting area, such that there was little overlap between structures. This helped to ensure that all structures inside the counting area were accounted for.

Using this optimized development assay procedure, the development of wild type *D. discoideum* and the DdiTLP2Δ strain were compared. The development of DdiTLP2Δ had not been previously described, although there is a replicable and statistically significant vegetative growth defect observed for the DdiTLP2Δ when compared to wild type *D. discoideum*. This was the only difference observed between the two strains, as other previous qualitative assessments of DdiTLP2Δ had been inconclusive. Cells from either strain looked the same under a microscope, both in shape and translucence. The vegetative growth defect suggested that there may also be a development defect, and this was confirmed by the development assay. This defect was only statistically significant at lower concentrations, as the defect was still present at higher concentrations but was not statistically significant.

It is unclear why this defect is only significant at lower concentrations. There is no difference in growth rate when the cells are at high concentration or at low concentration when grown in

media. As such, it is somewhat puzzling that there is a developmental defect associated with DdiTLP2Δ that can be readily observed at low concentrations but no such defect at high concentrations. This may be because of the aggregation in development. The larger structures and shorter chemotaxis distances that are present at high concentrations may help the DdiTLP2Δ strain recover some aspect of development, as the high concentration of cells may overcome the defect observed at lower concentrations. The lack of statistical significance may also be the result of experimental error, as the larger structures formed at these concentrations may have obscured additional structures in the counting area. There may have also been a more significant defect earlier in development, as only the endpoint of the assay was able to be analyzed under these conditions, due to the rapid time frame for development to occur.

The developmental defect for the DdiTLP2Δ strain seen at lower concentrations is likely rooted in the same reason that there was a vegetative growth defect when grown in rich liquid media. The DdiTLP2Δ cells are proven to grow slower than wild type cells, so this defect was also expected to be observed in development. Still, this is the only difference between the wild type cells and the DdiTLP2Δ cells. As can be seen in Figures 6B and C, there is no clear qualitative difference between the two – each structure in each stage of development looks similar for each strain. This result provides additional insight to the role of DdiTLP2 inside the cell. It has been previously confirmed that the G_{-1} addition to mt-tRNA^{His} is not strictly essential, suggesting that the HisRS in the mitochondria of *D. discoideum* is able to aminoacylate enough mt-tRNA^{His} over time to produce a viable cell. The growth and development defect demonstrated by DdiTLP2Δ may be related to less efficient aminoacylation or may be due to another effect of DdTLP2 entirely. It would be interesting for future studies to focus on the role of the mitochondrial HisRS, analyzing the specific region of the mt-tRNA^{His} that it recognizes prior to

aminoacylation. Specifically, the binding region should be compared between mt-$tRNA^{His}$ that contains G_{-1} or does not.

Conclusion and Future Studies

Canonical DNA and RNA biosynthesis is restricted to propagating nucleic acid synthesis in the 5’ to 3’ direction. However, the discovery that a G_{-1} nucleotide can be added to the 5’-end of $tRNA^{His}$ by the enzyme Thg1 revealed that nucleotide addition in the opposite (3'-5') direction is also possible. Further research into Thg1 revealed the Thg1 superfamily of enzymes that are all capable of this 3’-5’ nucleotide addition. One organism in particular, *D. discoideum*, contains a Thg1 enzyme and 3 TLPs. This work focused on characterizing one of these TLPs, DdiTLP2, using immunoprecipitation. A Flag tag was added to DdiTLP2 for these immunoprecipitations, and the activity of these enzymes was assessed. The best terminus for addition of this tag was unknown, so addition of the tag to each terminus was attempted. Only C-terminal Flag tagged DdiTLP2 was successfully synthesized and purified for *in vitro* analysis, and the presence of the Flag tag was confirmed using a western blot. To determine the activity of the enzyme, a phosphatase protection assay was completed, where a 22-fold defect in activity for C-terminal Flag tagged DdiTLP2 was observed when compared to wild type DdiTLP2. For *in vivo* analysis, only N-terminal Flag tagged DdiTLP2 was successfully cloned. It was subsequently electroporated into the DdiTLP2Δ strain, where expression of this protein was observed but the vegetative growth defect was not recovered. This suggests that the addition of an epitope tag onto this terminal end of the protein results in a significant activity defect that is not overcome by excess protein in the cell. The development of wild type *D. discoideum* and the DdiTLP2Δ strain were also characterized, where a statistically significant developmental defect was observed for DdiTLP2Δ.

Future studies into Flag tagged DdiTLP2 should focus on synthesizing C-terminal Flag tagged DdiTLP2 for *in vivo* studies. Since we have learned that N-terminal Flag tagged DdiTLP2 is not

sufficiently effective in the cell, it would be unnecessary to complete *in vitro* studies on this enzyme at this point. Preliminary work into the synthesis of C-terminal Flag tagged DdiTLP2 has led to a restriction cloning protocol that shows promise for generating the correct sequence. If this cloning is successful, a growth curve, development assay, and western blot should be completed for determine the efficiency of the epitope tagged enzyme *in vivo*. If the vegetative growth defect is recovered with the C-terminal Flag tagged DdiTLP2, the enzyme should be crosslinked and immunoprecipitated to determine if any proteins are interacting with DdiTLP2 during the catalysis of G_{-1} addition. The success of the tagging procedure would also lead to a similar epitope tagging procedure for other TLPs, especially DdiTLP4 since its function is still unknown.

Materials and Methods

C-Terminal Flag Tagged DdiTLP2 Expression and Purification

In previous work in our laboratory, the DdiTLP2 gene was cloned into an AVA-421 plasmid. This plasmid contains an ampicillin resistance gene, an N-terminal His_6 tag, and an IPTG inducible promoter for overexpression. Using this gene from our lab, Phusion PCR was used to add a C terminal Flag tag amplify the resulting gene. Following restriction digests by EcoRI and PstI to provide an initial confirmation of the sequence, the genes were sent to DNA sequencing to confirm addition of the C terminal Flag tag. The resulting gene was transformed into Rosetta pLysS cells, which is a strain of *E. coli* designed for protein expression. IPTG was used to induce overexpression in these cells, and the protein was purified using an immobilized metal ion affinity chromatography. The protein size and purity were confirmed using an SDS-PAGE gel. The concentration of the purified protein was determined using a Bradford assay.

Western Blot

To confirm the activity of the Flag tag on the C-terminal of DdiTLP2 or to confirm the expression of N-terminal Flag tag DdiTLP2 in *D. discoideum*, we utilized western blots. For this, a titration of the protein of interest, control proteins for the Flag tag, and ladders were ran on an SDS-PAGE gel. These proteins were then transferred to a nitrocellulose membrane by electrophoresis. The buffer in this electrophoresis was composed of 28.80 g of Tris base and 6.04 g of glycine dissolved in 1.8 L of water and 0.2 L of methanol. This transfer membrane was visualized using an Ponceau stain, where all proteins on the membrane can be seen. After removing the stain, the membrane is shaken in 4% nonfat milk for at least 3 hours. The primary antibody is then added to the new milk and shaken for at least 3 hours. The same is done for the

secondary antibody. The antibodies are then visualized using an ECL kit. The membrane is exposed to film, where the exposure time varies depending on activity of the antibodies.

Phosphatase Protection Assay

In previous work, the phosphatase protection assay has been developed to determine the efficiency of Thg1 and TLP nucleotide addition to $tRNA^{His}$ [11,23]. Two different types of this assay were completed in this work, endpoint assays and time course assays. For the endpoint assays, a titration of the DdiTLP2 enzyme was added to 5'-^{32}P labeled mt-$tRNA^{His}$ missing the G_{-1} nucleotide. The reaction is quenched after 2 hours by addition of RNase A. A phosphatase originating in cows (CIP) is then used to remove the 5' phosphate on each mt-$tRNA^{His}$. The products are resolved on a silica TLC overnight in a 55:35:10 (v:v:v; n-propanol:NH_4OH:H_2O) solvent system. These TLC plates were visualized by a Typhoon Trio phosphorimager and quantified using ImageQuant. The time course assays were completed similarly to the endpoint assays, except a constant concentration of DdiTLP2 was used and the reaction was quenched at set time points in the reaction. The time courses of product formation were plotted and fit to a single exponential rate equation in Kaleidagraph (Synergy Software). For time courses that did not fit this equation, the method of linear initial rates was used[38].

Growth of *D. discoideum*

In previous work in our laboratory, *D. discoideum* was frozen in the -80 °C freezer for long term storage. These cells are frozen in a solution of HL5 media with no antibiotics and DMSO in a 9:1 ratio[36,39]. For growth, the cells are quickly thawed in a warm water bath until a small amount of ice remains and subsequently added to a 10 cm petri dish containing 10 mL of HL5 media[36,39]. After the cells are allowed to recover at room temperature for 1 hour, they are centrifuged at

500 xg for 10 minutes at 4 °C[36,39]. A new 10 mL of HL5 media is then used to resuspend the cells for growth at 21 °C, the temperature for all subsequent growth. This process of centrifugation and resuspension in new media is used any time the media needs to be changed. Following this first night of growth, the media is changed into HL5 media containing ampicillin and streptomycin. From this point forward, the growth of the *D. discoideum* cells is checked daily. The cells are counted using a hemacytometer, where they are diluted as necessary to ease the counting burden. This is done to ensure that the concentration of cells is always between 5×10^4 and 4×10^6 cells/mL. If the cells have grown to the top of this range, they are pelleted and resuspended using the previous protocol, and a fraction of the resuspended pellet is used. The fraction is calculated such that the new concentration is always 5×10^4 cells/mL.

Electroporation of *D. discoideum*

The typical transformation processes used for *E. coli* are not effective for *D. discoideum*; as a result, electroporation is used for transformations in this system[39]. For electroporation, electrocompetent cells must be prepared from our strains of interest. These cells are harvested, centrifuged at 500x g for 10 minutes at 4 °C, then resuspended with a Na_3PO_4 buffer. The cells are then centrifuged again at the same speed and resuspended in ice cold HL50 buffer to a final concentration of 1×10^7 cells/mL. The cells are now electrocompetent. 10 μg of the DNA to be transformed is then added to 700 μL of these cells in a sterile 4 mm electroporation cuvette on ice. Using a Biorad X cell gene pulser, the cells are electroporated using the preset Dictyostelium settings (V = 1.0 kV, 10 μF, 1.0 ms pulse length, two pulses, 5-s pulse interval). The electroporated cells are then quickly added to 1 mL of HL5 media in a petri dish and shaken at 40 RPM for 15 minutes at room temperature. Cold solutions of $CaCl_2$ and $MgCl_2$ are then added

to final concentrations of 2 mM each, and the dish is again shaken at 40 RPM for 15 minutes at room temperature. The resulting cells are added to 11 mL of HL5 media for growth overnight at 21 °C. The media is changed the next day to 10 mL of HL5 media with ampicillin and streptomycin.

Development Assay of *D. discoideum*

To assess the development of *D. discoideum*, previously described development assays were used to optimize the assay for DdiTLP2Δ[36]. For this assay, 2 x 10^7 cells were grown for subsequent plating. These cells were grown according to the procedures described above. After determining the number of cells grown, the cells were pelleted and resuspended in 10 mL of DB buffer. This solution was then split such that 4 tubes were generated. The tubes contained 1 x 10^7, 5 x 10^6, 2.5 x 10^6, and 1 x 10^6 cells, respectively. These tubes were all centrifuged and resuspended in 3 mL of DB buffer twice. After the second resuspension, the cells are centrifuged again and resuspended in 200 μL of DB buffer. This solution is plated onto a nutrient poor KK2 plate and spread evenly with a sterile glass spreader. The plate is wrapped in a wet paper towel and placed in a resealable zipper storage bag for development at 21 °C. The cells are allowed to develop for 7 days, after which they are photographed using an Olympus SZX16 microscope. Six pictures of each plate are taken. Due to software issues with this microscope – the scale bar did not change with the zoom of the microscope – all plates were photographed using the same settings to ensure the scale bar was standardized. The bottom light was set to max brightness, an additional LED lamp was set to 1.3, the exposure was set to $^1/_{200}$ second, the objective used was 1.25x, the sensitivity was ISO 200, and the zoom was set to 1.6x. A 3 x 3 mm square is used for counting the structures on each picture to reduce the counting burden.

Lysing of *D. discoideum* cells

For Western blotting and immunoprecipitations, the *D. discoideum* cells are lysed by sheer force using a steel ball cell cracker[40]. The balls used here are 8.002 mm in diameter. After counting the cells, they are pelleted and resuspended in 1 mL of cell cracker buffer. This is done to maximize the concentration of the solution when passed through the cell cracker. A 5 mL syringe is used to draw up this solution and it is passed through the cell cracker 10-15 times. Intact cells are then removed by centrifugation at 1,200 xg for 5 minutes. The supernatant is stored for future studies.

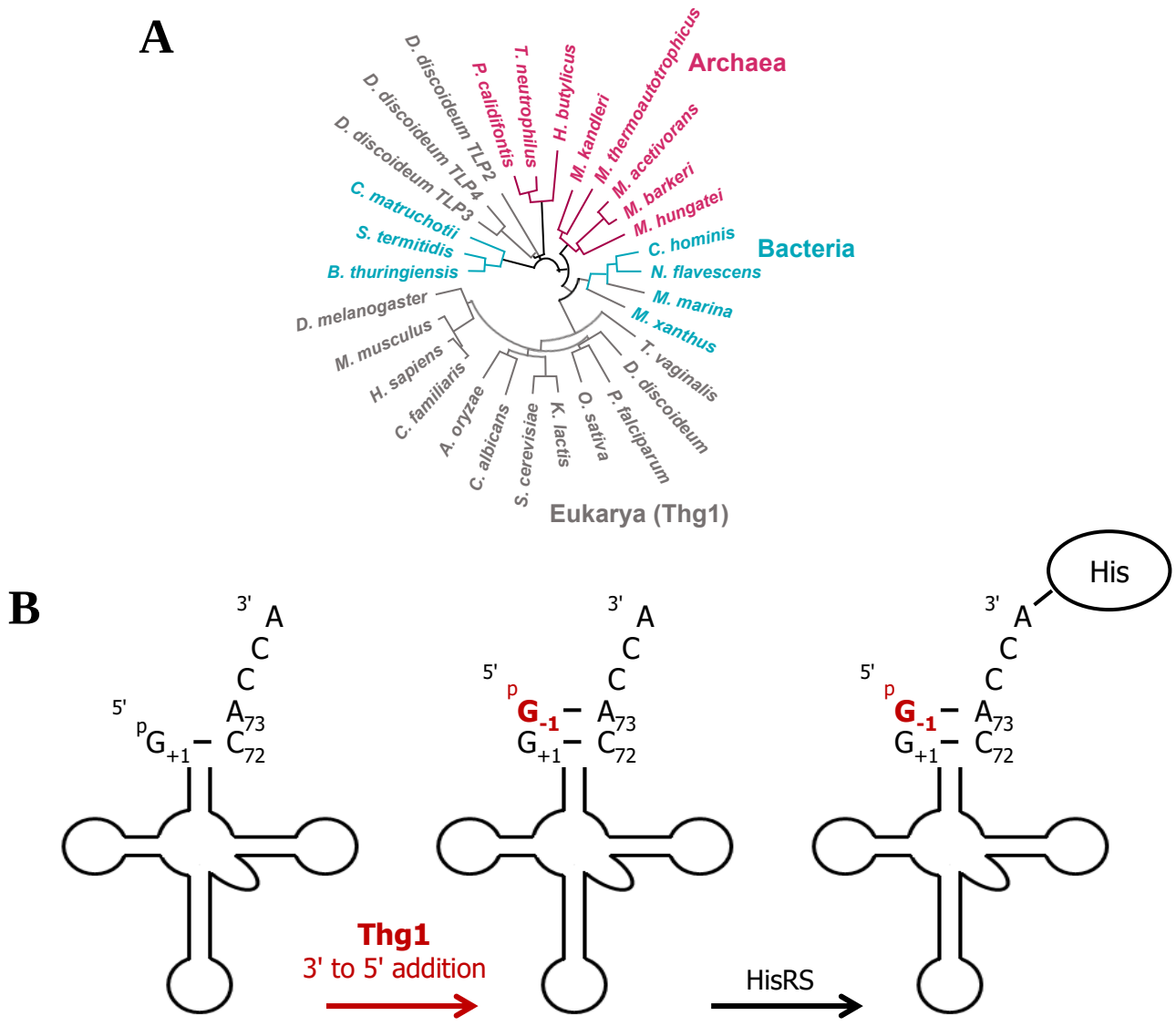

Figure 1: Phylogeny of Thg1 Superfamily (A) A phylogenetic analysis of the Thg1 superfamily showing Thg1 and DdiTLP phylogeny. Thg1 is shown to contain similarities across domain of life. (B) The specific addition of G_{-1} catalyzed by Thg1 and its role in the greater aminoacylation process.

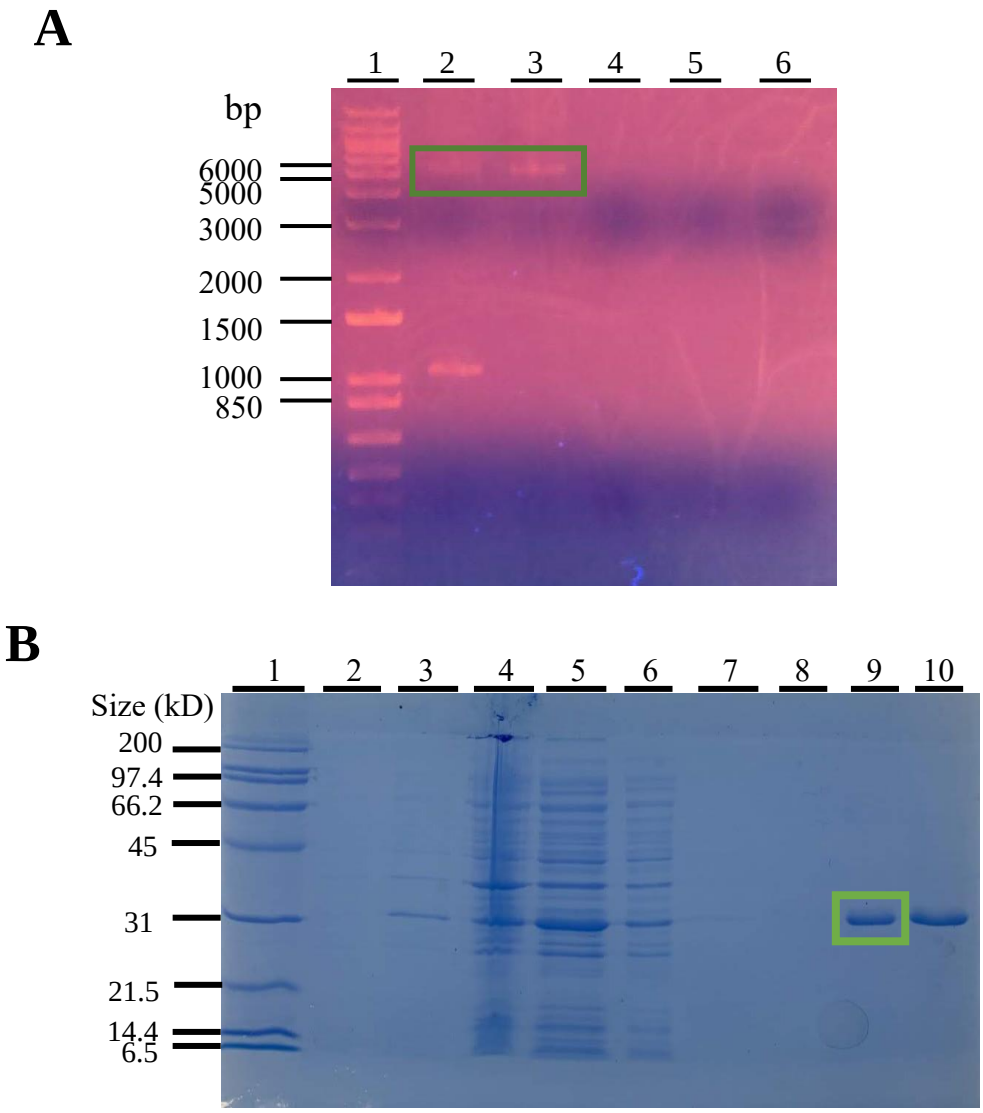

Figure 2: Cloning and Purification of C-terminal Flag DdiTLP2 (A) A 1% agarose gel after Phusion PCR of N and C terminal Flag DdiTLP2. Lanes 2 and 3 contain N-terminal Flag DdiTLP2 and C-terminal Flag DdiTLP2, respectively, where the expected band is outlined in the green box. Lanes 4 and 5 contain no template DNA, where N-terminal primers were used in lane 4 and C-terminal primers were used in lane 5. Lane 6 contains no primers. (B) An SDS-PAGE gel after purification of C-terminal Flag DdiTLP2, where the expected size was 32 kD. Lanes 2-10 include: pre-induction sample, post-induction sample, pre-lysis, crude extract, flow through, wash 1, wash 2, purified C-terminal DdiTLP2, TALON resin.

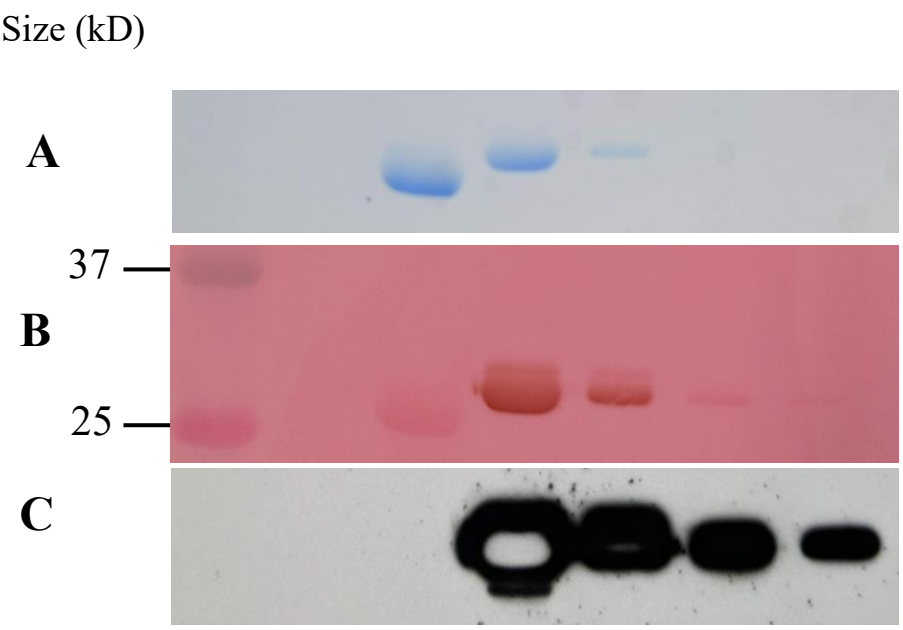

Figure 3: Western Blot of C terminal Flag DdiTLP2 (A) The Coomassie stained SDS-PAGE gel following protein transfer to the membrane. (B) The Ponceau stained nitrocellulose membrane following transfer of proteins. (C) The exposure pattern of the interaction between anti-Flag-HRP and C terminal Flag DdiTLP2. Lane 2 is a positive control of yTrm10 Flag that did not show up. Lane 3 is a negative control of wild type DdiTLP2. Lanes 4-7 are a titration in concentration of C terminal Flag DdiTLP2.

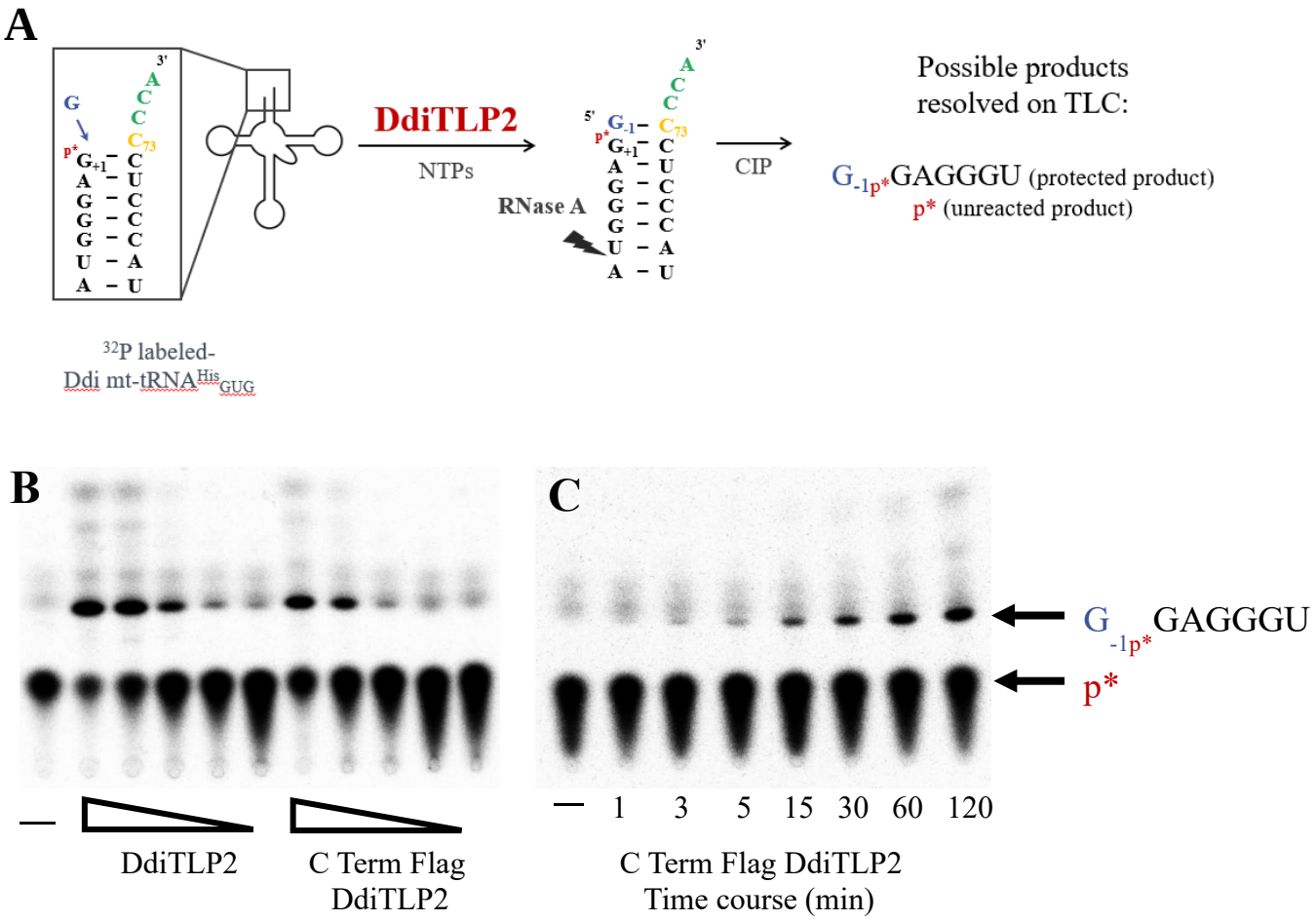
A
DdiTLP2
NTPs
RNase A
CIP
Possible products resolved on TLC:
G-1p*GAGGGU (protected product)
p* (unreacted product)
32P labeled-
Ddi mt-tRNAHisGUG
B
DdiTLP2
C Term Flag DdiTLP2
C
G-1p*GAGGGU
p*
1 3 5 15 30 60 120
C Term Flag DdiTLP2 Time course (min)

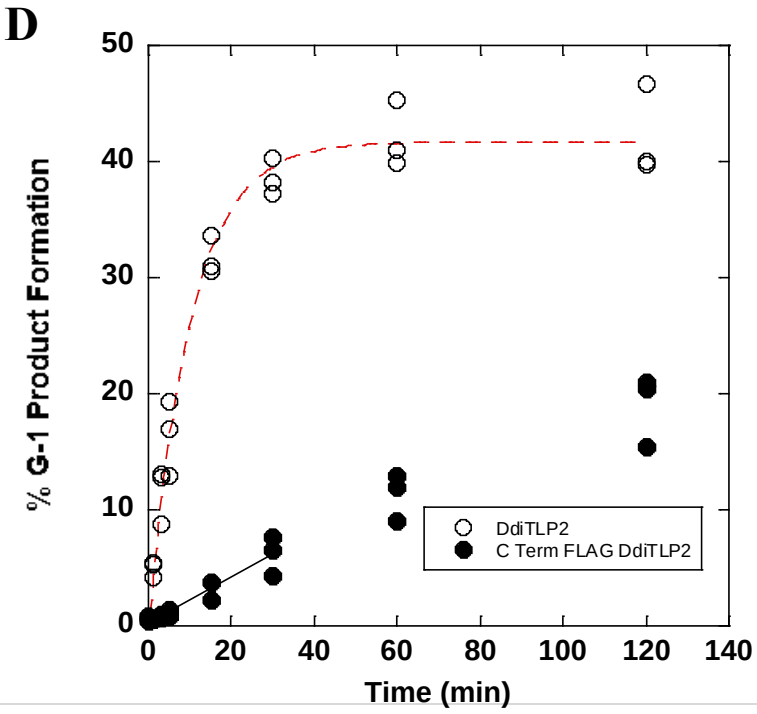
D
% G-1 Product Formation
Time (min)
DdiTLP2
C Term FLAG DdiTLP2

E

Substrate	Enzyme	k_{obs} (min^{-1})
Ddi mt-tRNA^{His} G_{+1}	DdiTLP2	0.099 ± 0.007
	C Term FLAG DdiTLP2	0.0046

n=3
DdiTLP2 data fit to single exponential
DdiTLP2 FLAG analyzed with method of linear initial rates
[E] = 3 μM final concentration, [E] > [S]

Figure 4: Phosphatase Protection Assay of C term Flag DdiTLP2 (A) A schematic for the phosphatase protection assay. DdiTLP2 adds a G_{-1} nucleotide to the 5' end of Ddi mt-tRNA$^{His}_{GUG}$, protecting the ^{32}P G_{+1} nucleotide. The reaction is then quenched by RNase A followed by phosphatase digestion removing the 5' phosphate group. The products are then resolved by silica TLC. (B) A representative TLC scan of an endpoint assay of DdiTLP2 activity on mt-tRNA^{His} after RNase A digestion. Spots correlating to G_{-1} addition and unreacted phosphate are labeled. The activity of the enzyme is confirmed by the disappearance of the G_{-1} spot with removal of DdiTLP2. (C) A representative TLC scan of a time course assay of DdiTLP2 activity on mt-tRNA^{His} after RNase A digestion. The activity of the enzyme is confirmed by the appearance of the G_{-1} spot over time. (D) The time courses from (C) are plotted here, where formation of the G_{-1} product is plotted against time. (E) The data from DdiTLP2 fits a single exponential, and the k_{obs} was taken directly from this. The method of linear initial rates was used to calculate the k_{obs} for FLAG tagged DdiTLP2. A 22-fold defect in activity for FLAG tagged DdiTLP2 was calculated.

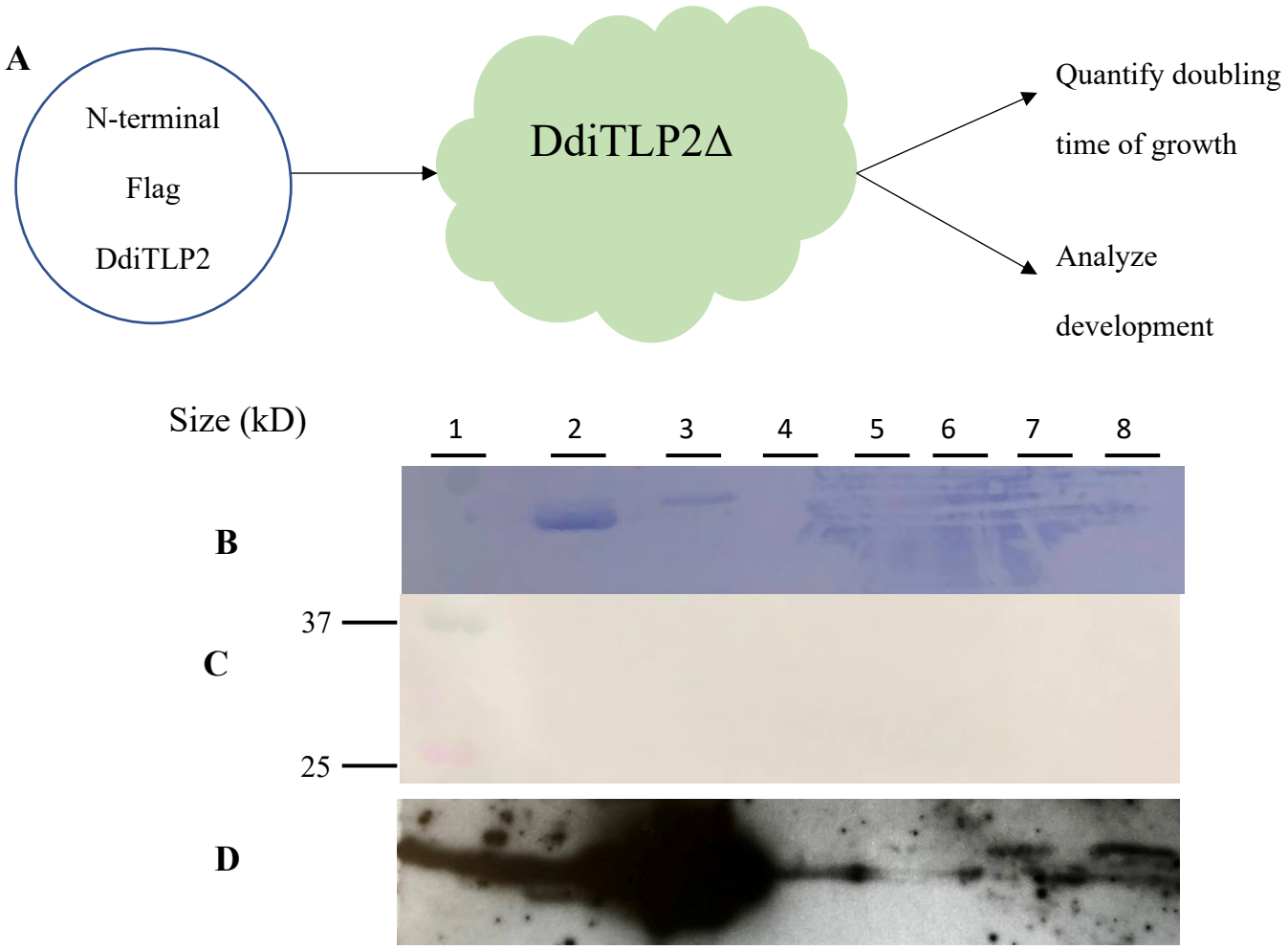

Figure 5: Western Blot of N-terminal Flag DdiTLP2 (A) The workflow of the *in vivo* analysis of N-terminal Flag DdiTLP2. (B) The Coomassie stained SDS-PAGE gel following protein transfer to the membrane. (C) The Ponceau stained nitrocellulose membrane following transfer of proteins. (D) The exposure pattern of the interaction between anti-Flag-HRP and N-terminal Flag DdiTLP2. Lane 2 is a negative control wild type DdiTLP2. Lane 3 is a positive control of C-terminal Flag DdiTLP2. Lanes 4-7 are an increasing titration in concentration of cell extract from cells containing N-terminal Flag DdiTLP2. Lane 8 contains uncracked cells containing N-terminal Flag DdiTLP2.

A

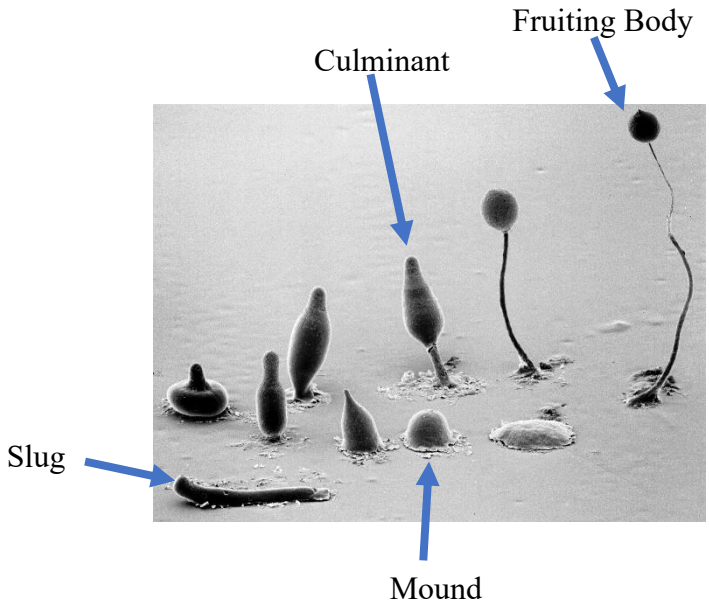

B

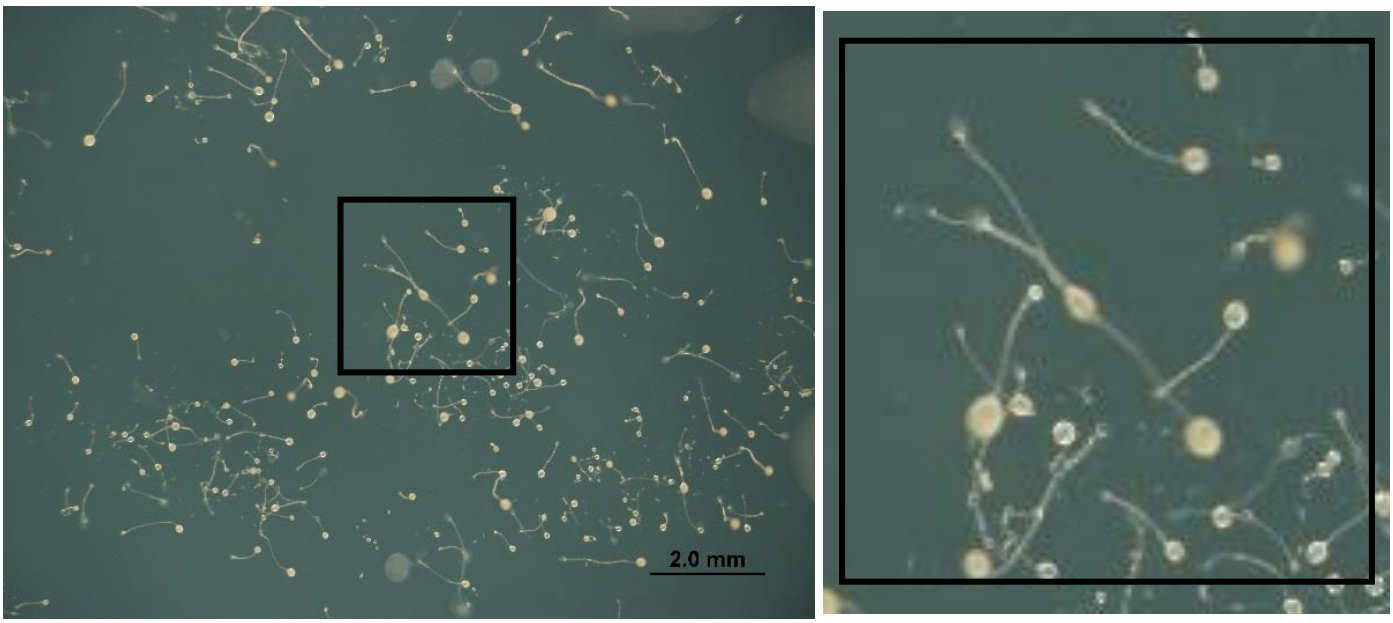

C

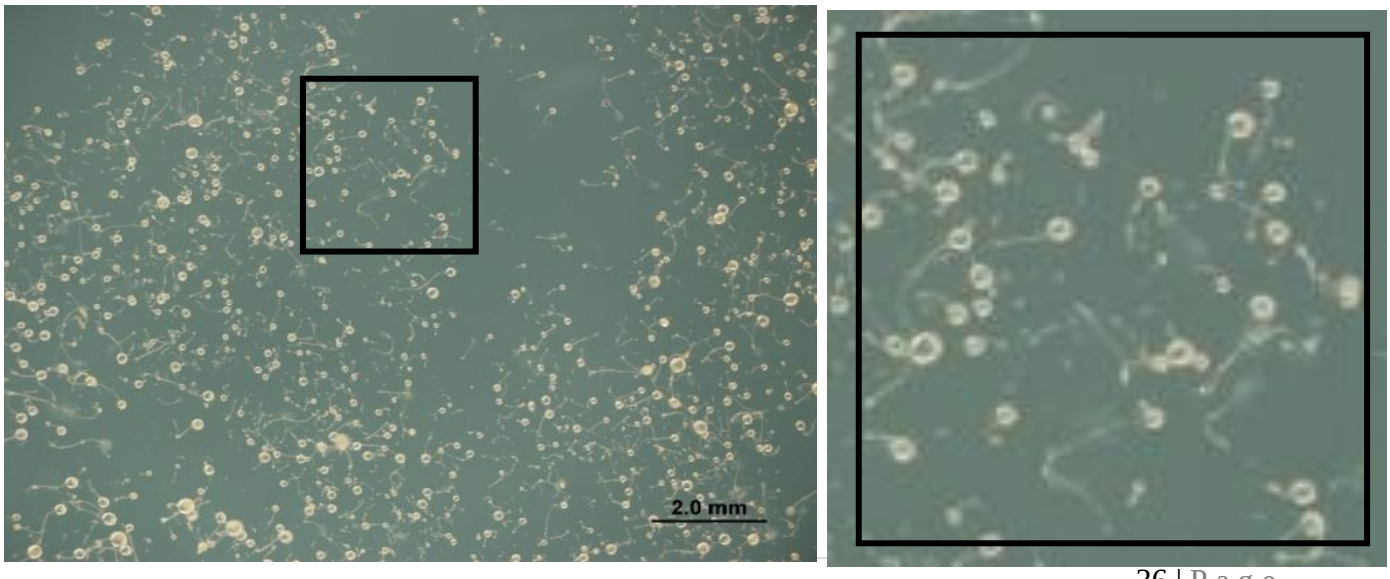

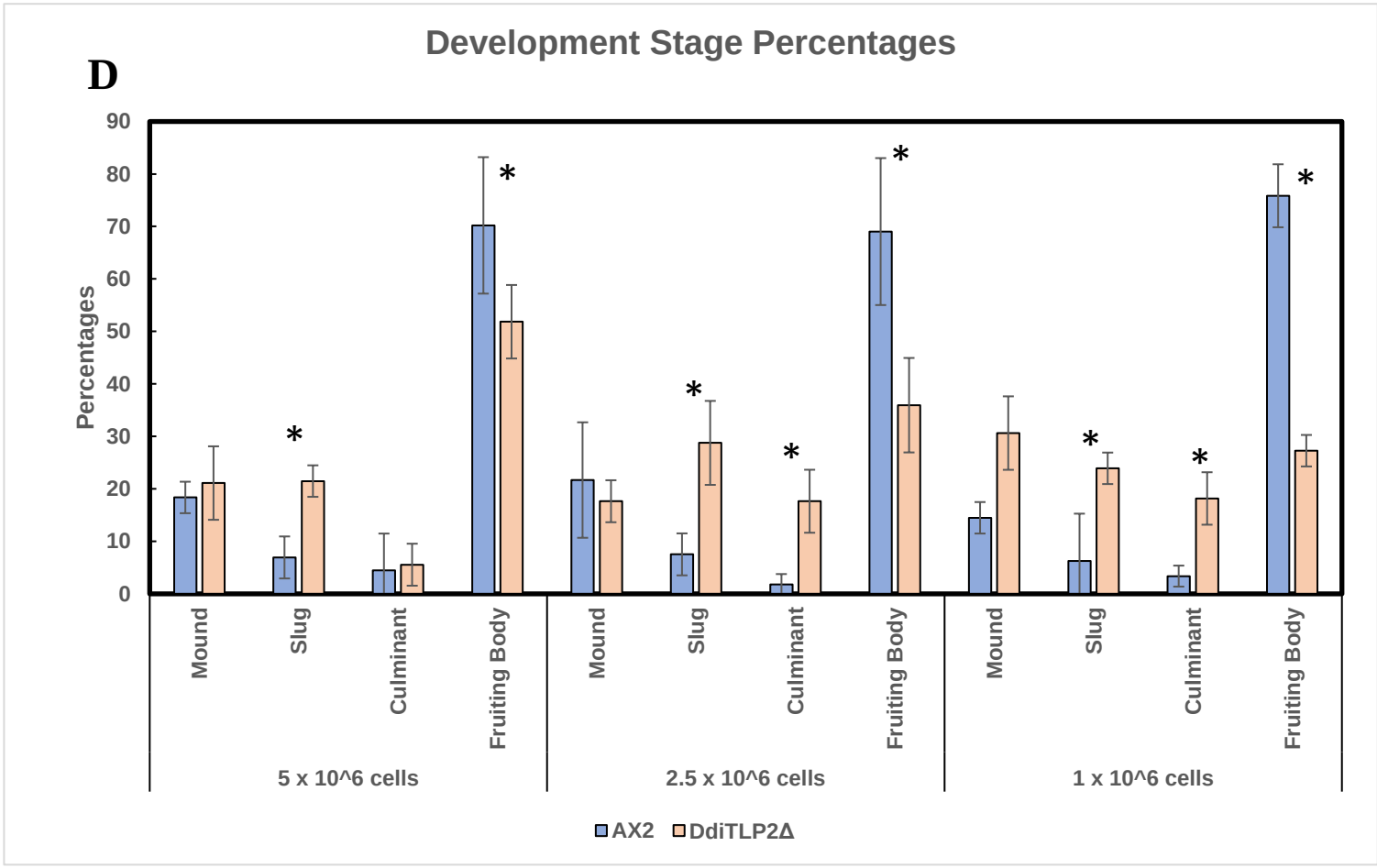

Figure 6: Development of Assay of *D. discoideum* and the DdiTLP2Δ strain.

(A) Representative images for each stage in development counted in the development assay. Picture is used with permission from M.J. Grimson and R.L. Blanton from Texas Tech University. (B) A representative microscope image of the development assay after 1 week of growth. There were 5 x 10^6 AX2 cells plated on this plate. The 3 mm by 3 mm square was used for counting. (C) A representative microscope image of the development assay after 1 week of growth. There were 5 x 10^6 DdiTLP2Δ cells plated on this plate. The 3 mm by 3 mm square was used for counting. (D) The percentage of cells on each plate that reached each major developmental stage. The data is split by cell type and number of cells on the plate. Significant developmental defects are seen at 2.5 x 10^6 and 1 x 10^6 cells, where wild type AX2 cells reach later developmental stages faster than DdiTLP2Δ cells. The asterisks indicate statistical significance from a chi squared test.

References

1. Cooley L, Appel B, Soll D. Post-transcriptional nucleotide addition is responsible for the formation of the 5' terminus of histidine tRNA. *Proceedings of the National Academy of Sciences*. 1982;79(21):6475-6479. doi:10.1073/pnas.79.21.6475
2. Gu W, Hurto RL, Hopper AK, Grayhack EJ, Phizicky EM. Depletion of Saccharomyces cerevisiae tRNAHis Guanylyltransferase Thg1p Leads to Uncharged tRNAHis with Additional m5C. *Mol Cell Biol*. 2005;25(18):8191-8201. doi:10.1128/MCB.25.18.8191-8201.2005
3. Connolly SA, Rosen AE, Musier-Forsyth K, Francklyn CS. G-1:C73 recognition by an arginine cluster in the active site of Escherichia coli histidyl-tRNA synthetase. *Biochemistry*. 2004;43(4):962-969. doi:10.1021/bi035708f
4. Himeno H, Hasegawa T, Ueda T, Watanabe K, Miura K, Shimizu M. Role of the extra G-C pair at the end of the acceptor stem of tRNA(His) in aminoacylation. *Nucleic Acids Res*. 1989;17(19):7855-7863.
5. Rosen AE, Brooks BS, Guth E, Francklyn CS, Musier-Forsyth K. Evolutionary conservation of a functionally important backbone phosphate group critical for aminoacylation of histidine tRNAs. *RNA*. 2006;12(7):1315-1322. doi:10.1261/rna.78606
6. Rudinger J, Florentz C, Giegé R. Histidylation by yeast HisRS of tRNA or tRNA-like structure relies on residues -1 and 73 but is dependent on the RNA context. *Nucleic Acids Res*. 1994;22(23):5031-5037. doi:10.1093/nar/22.23.5031
7. Howell NW, Jackman JE. Impact of Chemical Modification on tRNA Function. In: *ELS*. American Cancer Society; 2019:1-11. doi:10.1002/9780470015902.a0028527

8. Jackman JE. tRNA Biogenesis. In: *ELS*. American Cancer Society; 2010. doi:10.1002/9780470015902.a0020894
9. Betat H, Long Y, Jackman JE, Mörl M. From End to End: tRNA Editing at 5'- and 3'-Terminal Positions. *Int J Mol Sci*. 2014;15(12):23975-23998. doi:10.3390/ijms151223975
10. Gu W, Jackman JE, Lohan AJ, Gray MW, Phizicky EM. tRNAHis maturation: An essential yeast protein catalyzes addition of a guanine nucleotide to the 5′ end of tRNAHis. *Genes Dev*. 2003;17(23):2889-2901. doi:10.1101/gad.1148603
11. Jackman JE, Phizicky EM. tRNAHis guanylyltransferase catalyzes a 3′-5′ polymerization reaction that is distinct from G−1 addition. *Proc Natl Acad Sci U S A*. 2006;103(23):8640-8645. doi:10.1073/pnas.0603068103
12. Jackman JE, Gott JM, Gray MW. Doing it in reverse: 3′-to-5′ polymerization by the Thg1 superfamily. *RNA*. 2012;18(5):886-899. doi:10.1261/rna.032300.112
13. Abad MG, Long Y, Willcox A, Gott JM, Gray MW, Jackman JE. A role for tRNAHis guanylyltransferase (Thg1)-like proteins from Dictyostelium discoideum in mitochondrial 5′-tRNA editing. *RNA*. 2011;17(4):613-623. doi:10.1261/rna.2517111
14. Rao BS, Maris EL, Jackman JE. tRNA 5′-end repair activities of tRNAHis guanylyltransferase (Thg1)-like proteins from Bacteria and Archaea. *Nucleic Acids Res*. 2011;39(5):1833-1842. doi:10.1093/nar/gkq976
15. Orellana O, Cooley L, Söll D. The additional guanylate at the 5' terminus of Escherichia coli tRNAHis is the result of unusual processing by RNase P. *Mol Cell Biol*. 1986;6(2):525-529. doi:10.1128/mcb.6.2.525

16. Jühling F, Mörl M, Hartmann RK, Sprinzl M, Stadler PF, Pütz J. tRNAdb 2009: compilation of tRNA sequences and tRNA genes. *Nucleic Acids Res*. 2009;37(Database issue):D159-162. doi:10.1093/nar/gkn772
17. Abad MG, Rao BS, Jackman JE. Template-dependent 3′–5′ nucleotide addition is a shared feature of tRNAHis guanylyltransferase enzymes from multiple domains of life. *Proc Natl Acad Sci U S A*. 2010;107(2):674-679. doi:10.1073/pnas.0910961107
18. Hyde SJ, Rao BS, Eckenroth BE, Jackman JE, Doublié S. Structural Studies of a Bacterial tRNAHIS Guanylyltransferase (Thg1)-Like Protein, with Nucleotide in the Activation and Nucleotidyl Transfer Sites. *PLoS One*. 2013;8(7). doi:10.1371/journal.pone.0067465
19. Hyde SJ, Eckenroth BE, Smith BA, et al. tRNA(His) guanylyltransferase (THG1), a unique 3'-5' nucleotidyl transferase, shares unexpected structural homology with canonical 5'-3' DNA polymerases. *Proc Natl Acad Sci U S A*. 2010;107(47):20305-20310. doi:10.1073/pnas.1010436107
20. Smith BA, Jackman J. Kinetic analysis of 3'-5' nucleotide addition catalyzed by eukaryotic tRNA(His) guanylyltransferase. *Biochemistry*. Published online 2012. doi:10.1021/bi201397f
21. Nakamura A, Nemoto T, Heinemann IU, et al. Structural basis of reverse nucleotide polymerization. *Proc Natl Acad Sci U S A*. 2013;110(52):20970-20975. doi:10.1073/pnas.1321312111
22. Long Y, Abad MG, Olson ED, Carrillo EY, Jackman JE. Identification of distinct biological functions for four 3′-5′ RNA polymerases. *Nucleic Acids Research*. 2016;44(17):8395-8406. doi:10.1093/nar/gkw681

23. Jackman JE, Phizicky EM. tRNAHis guanylyltransferase adds G−1 to the 5′ end of tRNAHis by recognition of the anticodon, one of several features unexpectedly shared with tRNA synthetases. *RNA*. 2006;12(6):1007-1014. doi:10.1261/rna.54706
24. Lonergan KM, Gray MW. Editing of transfer RNAs in Acanthamoeba castellanii mitochondria. *Science*. 1993;259(5096):812-816. doi:10.1126/science.8430334
25. Lonergan KM, Gray MW. Predicted editing of additional transfer RNAs in Acanthamoeba castellanii mitochondria. *Nucleic Acids Res*. 1993;21(18):4402.
26. Price DH, Gray MW. A novel nucleotide incorporation activity implicated in the editing of mitochondrial transfer RNAs in Acanthamoeba castellanii. *RNA*. 1999;5(2):302-317.
27. Preston MA, Phizicky EM. The requirement for the highly conserved G−1 residue of Saccharomyces cerevisiae tRNAHis can be circumvented by overexpression of tRNAHis and its synthetase. *RNA*. 2010;16(5):1068-1077. doi:10.1261/rna.2087510
28. Rice TS, Ding M, Pederson DS, Heintz NH. The Highly Conserved tRNAHis Guanylyltransferase Thg1p Interacts with the Origin Recognition Complex and Is Required for the G2/M Phase Transition in the Yeast Saccharomyces cerevisiae. *Eukaryot Cell*. 2005;4(4):832-835. doi:10.1128/EC.4.4.832-835.2005
29. Guo D, Hu K, Lei Y, Wang Y, Ma T, He D. Identification and Characterization of a Novel Cytoplasm Protein ICF45 That Is Involved in Cell Cycle Regulation *. *Journal of Biological Chemistry*. 2004;279(51):53498-53505. doi:10.1074/jbc.M406737200
30. Murphy M, Hickey F, Godson C. IHG-1 amplifies TGF-β1 signalling and mitochondrial biogenesis and is increased in diabetic kidney disease. *Curr Opin Nephrol Hypertens*. 2013;22(1):77-84. doi:10.1097/MNH.0b013e32835b54b0

31. Murphy M, Godson C, Cannon S, et al. Suppression subtractive hybridization identifies high glucose levels as a stimulus for expression of connective tissue growth factor and other genes in human mesangial cells. *J Biol Chem*. 1999;274(9):5830-5834. doi:10.1074/jbc.274.9.5830
32. Clarkson MR, Murphy M, Gupta S, et al. High glucose-altered gene expression in mesangial cells. Actin-regulatory protein gene expression is triggered by oxidative stress and cytoskeletal disassembly. *J Biol Chem*. 2002;277(12):9707-9712. doi:10.1074/jbc.M109172200
33. Hickey FB, Corcoran JB, Docherty NG, et al. IHG-1 promotes mitochondrial biogenesis by stabilizing PGC-1α. *J Am Soc Nephrol*. 2011;22(8):1475-1485. doi:10.1681/ASN.2010111154
34. Corcoran JB, McCarthy S, Griffin B, et al. IHG-1 must be localised to mitochondria to decrease Smad7 expression and amplify TGF-β1-induced fibrotic responses. *Biochimica et Biophysica Acta (BBA) - Molecular Cell Research*. 2013;1833(8):1969-1978. doi:10.1016/j.bbamcr.2013.03.027
35. Brizzard B. Epitope tagging. *BioTechniques*. 2008;44(5):693-695. doi:10.2144/000112841
36. Fey P, Kowal AS, Gaudet P, Pilcher KE, Chisholm RL. Protocols for growth and development of Dictyostelium discoideum. *Nature Protocols*. 2007;2(6):1307-1316. doi:10.1038/nprot.2007.178
37. Driessche NV, Shaw C, Katoh M, et al. A transcriptional profile of multicellular development in Dictyostelium discoideum. *Development*. 2002;129(7):1543-1552.
38. Smith BA, Jackman JE. Saccharomyces cerevisiae Thg1 Uses 5′-Pyrophosphate Removal To Control Addition of Nucleotides to tRNAHis. *Biochemistry*. 2014;53(8):1380-1391. doi:10.1021/bi4014648

39. Gaudet P, Pilcher KE, Fey P, Chisholm RL. Transformation of Dictyostelium discoideum with plasmid DNA. *Nature Protocols*. 2007;2(6):1317-1324. doi:10.1038/nprot.2007.179
40. Bof M, Brandolin G, Satre M, Klein G. The mitochondrial adenine nucleotide translocator from Dictyostelium discoideum. *European Journal of Biochemistry*. 1999;259(3):795-800. doi:https://doi.org/10.1046/j.1432-1327.1999.00088.x